THE JOURNAL OF PHYSICAL CHEMISTRY B

Article

pubs.acs.org/JPCB

First Steps in the Aggregation Process of Copolymers Based on Thymine Monomers: Characterization by Molecular Dynamics Simulations and Atomic Force Microscopy

A. Sergio Garay,[†] Daniel E. Rodrigues,[*,†,‡] Antonela Fuselli,[†] Debora M. Martino,[§] and Mario C. G. Passeggi, Jr.[§,∥]

[†]Departamento de Física, Facultad de Bioquímica y Ciencias Biológicas, C.C. 242, Ciudad Universitaria, Universidad Nacional del Litoral (UNL), S3000ZAA Santa Fe, Argentina

[‡]Instituto de Desarrollo Tecnológico para la Industria Química (INTEC) and [§]Instituto de Física del Litoral (IFIS Litoral), CONICET-UNL, Güemes 3450, S3000GLN Santa Fe, Argentina

[∥]Departamento de Materiales, Facultad de Ingeniería Química, Universidad Nacional del Litoral (UNL), Santiago del Estero 2829, S3000AOM Santa Fe, Argentina

ABSTRACT: Atomistic molecular dynamic simulations were performed to study the structure of isolated VBT−VBA (vinylbenzylthymine−vinylbenzyltriethylammonium chloride) copolymer chains in water at different monomeric species ratios (1:1 and 1:4). The geometric parameters of the structure that the copolymers form in equilibrium together with the basic interactions that stabilize them were determined. Atomic force microscopy (AFM) measurements of dried diluted concentrations of the two copolymers onto highly oriented pyrolytic graphite (HOPG) substrates were carried out to study their aggregation arrangement. The experiments show that both copolymers arrange in fiber-like structures. Comparing the diameters predicted by the simulation results and those obtained by AFM, it can be concluded that individual copolymers arrange in bunches of two chains, stabilized by contra-ions−copolymer interactions for the 1:1 copolymerization ratio at the ionic strength of our samples. In contrast, for the 1:4 system the individual copolymer chains do not aggregate in bunches. These results remark the relevance of the copolymerization ratio and ionic strength of the solvent in the mesoscopic structure of these materials.

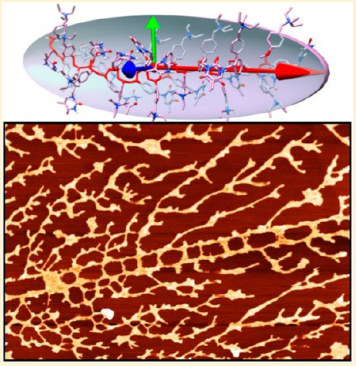

INTRODUCTION

A novel class of environmentally benign, nontoxic, and recyclable materials based on vinylbenzylthymine (VBT) and ionically charged vinylbenzyltriethylammonium chloride (VBA) monomers have been experimentally studied during the past 10 years[1−3] with the main goal of improving their synthesis and curing methods. Given the chemical structure of the copolymers, having various positively charged groups pending from their backbones, they can be considered as charged macro-ions, like polystyrenesulfonate, polyacrylic and polymethacrylic acids and their salts, DNA, and other polyacids and polybases. Electrostatic interactions dominate the internal conformational behavior (diluted copolymer solution) and also the interchain interactions (semidiluted polymer solution).[4] Consequently, it is beneficial to understand the molecular behavior of thymine copolymers in water using molecular dynamics (MD) simulations.

According to the different research goals, polyelectrolyte solutions have been modeled as an ensemble of bead−spring chains of charged Lennard-Jones particles with explicit counterions using MD simulations.[5,6] Nevertheless, the polycations have also been modeled as rod-like structures.[7] The solvent has been simulated using either implicit or explicit approaches (as bead without charge).[8,9] Full atomistic simulations of a variety of charged[10−12] and neutral[13,14] copolymers have been performed in some studies where the level of detail was necessary for their purposes.

The aim of this work is to understand the molecular behavior of these copolymers in water using molecular dynamics (MD) simulations and atomic force microscopy (AFM). To the best of our knowledge, this is the first study that describes the structure of the VBT−VBA charged copolymer species in quasi-full atomistic detail (united atom model) using MD simulations in explicit water. The simulation studies complement the experimental results of aqueous copolymers carried out in our laboratory.

To obtain a useful material for technological applications, the copolymer chains must undergo the "curing" process, where the long fibers obtained in the polymerization stage are cross-linked via photodimerization between adjacent thymine moieties upon UV irradiation. The cross-linking process requires a close contact among equally charged fibers which has been a matter

Received: November 19, 2015
Revised: March 18, 2016

DOI: 10.1021/acs.jpcb.5b11342
J. Phys. Chem. B XXXX, XXX, XXX−XXX

of debate and study in the past years.[15,16] It has become increasingly evident that only an accurate knowledge of the behavior of single copolymer chains in solution combined with a proper understanding of their aggregation behavior can ensure the well-controlled and reproducible material properties.[17] In this context, the copolymers were studied in both diluted and concentrated solutions, free of added salts. While the former simulations allowed us to understand the copolymer conformational behavior isolated from other copolymers, the second approach served to analyze how the copolymer chains interact among them in the aggregation process.

Correspondingly, the effect of the added solvation groups (VBA, positively charged) and its distribution along the chain backbone on the resulting conformational and solvation structure was investigated. Potential applications of the variety of ways copolymers intertwine using different concentrations of different contra-ions are promising.

MATERIALS AND METHODS

Parameters Development. *Charge Parametrization.* Suitable structures for each monomer in the copolymers to be modeled were built using the Tinker[18] package (Figure 1). A conformational search procedure was run (SCAN) for each structure in order to find their global minimum energy conformer (MM2 force field[19]). The partial charges for the atoms of these molecules were calculated with the program GAMESS-US[20] and RESP fitting. Electrostatic potentials calculated with the 6-31G* basis using RHF and geometry optimization were used for fitting the partial charges using the two-step RESP procedure.[21]

Bonding and Nonbonding Interactions. Parameters for the vinylbencyl moiety which is common to both VBT and VBA monomers were taken from the phenylalanine Gromos96 53a6 force field.[22] Thymine Gromos96 53a6 parameters were used for thymine moiety. The triethylammonium moiety was parametrized using the atom types applied by Chiu et al.[23] in the choline moiety of the dipalmitoylphosphatidylcholine (DPPC) molecule which includes united atoms by aliphatic carbons.[22] United atoms were also used to describe the CH_x groups of the copolymer backbone. Figure 1 shows the atom types and charges used for each monomer of the copolymers. The charged group of the VBA monomer is shown surrounded by a blue rectangle.

Molecular Dynamic Simulations. All MD simulations were performed using the Gromacs package version 4.5.[24−26] A direct cutoff for nonbonded interactions of 1 nm and particle mesh Ewald summation for long-range electrostatics were applied.[27] Berendsen baths[28] were used to couple the simulation boxes with an isotropic pressure of 1 atm and a reference temperature. The copolymers and water molecules were coupled to separate Berendsen thermostats with a relaxation time of 0.1 ps. All bond lengths were constrained using the LINCS algorithm[29] whereas the SETTLE algorithm[30] was used for water molecules. All the systems were solvated with SPC water molecules.[31] The time step in all the simulations was set to 2 fs. Trajectories were analyzed using the standard tools from the Gromacs package and custom-written tcl scripts for the VMD visualization package.[32]

Molecular Dynamic Protocol. The starting copolymers coordinates were built with an *ad hoc* tcl program, which assembles the monomers described above with a particular VBT:VBA ratio, assigning random dihedral angles for the backbone carbon atoms, in order to introduce some conformational randomness. Two copolymers having different ratios were built, a VBT:VBA 1:1 (containing 32 monomers) and a VBT:VBA 1:4 (containing 35 monomers), called hereafter Pol 1:1 and Pol 1:4, respectively.

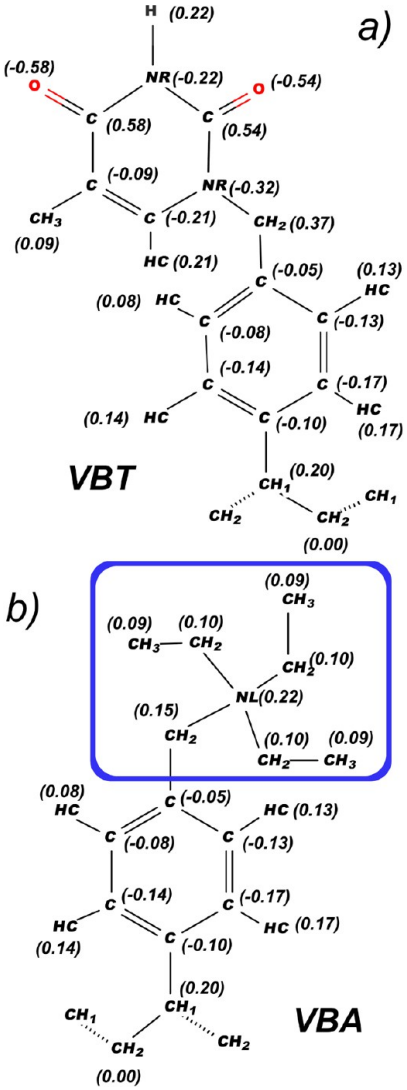

Figure 1. Partial charges (in parentheses) and Gromos96 53a6 atom type names used to describe the interactions of the VBT (a) and VBA (b) monomers for the MD simulations. The blue rectangle in (b) marks off the charged triethylammonium moiety. Aliphatic C groups of the charged moiety and of the copolymer's backbone are parametrized as united atoms in the force field.

In the MD simulations of the copolymers Pol 1:1 and Pol 1:4, only the ordered monomer sequences of $[\text{VBA-VBT-}]_n$ and $[(\text{VBA-})_4\text{VBT-}]_n$ were used, respectively. The length of the copolymer chains with an explicit solvent that can be simulated in an atomistic MD procedure, and the long relaxation times required to achieve the equilibrium state (see below) make unfeasible to deal with sequence disorder. This approach ignores the natural experimental disorder introduced in the free-radical copolymerization reactions; nevertheless, given the almost identical reactivities for each comonomer radicals observed for this system,[33] the method was considered a valid approximation to study the copolymer properties.

Based on these two copolymers, four systems were prepared: (1) an isolated Pol 1:1 in water, (2) an isolated Pol 1:4 in

DOI: 10.1021/acs.jpcb.5b11342
J. Phys. Chem. B XXXX, XXX, XXX−XXX

Table 1. Size of Simulated Systems

no. of molecules	Pol 1:1	Pol 1:4	2 × (Pol 1:1)	2 × (Pol 1:4)
water (SPC)	19321	21052	18625	21889
ions	16	28	32	56

water, (3) two Pol 1:1 chains in water, and (4) two Pol 1:4 chains in water.

Each copolymer, or couple of copolymers, was centered in an octahedral box and solvated with SPC water.[31] The distance of any copolymer atom to any border of the box was kept longer than 1 nm. A simulated annealing (SA) procedure was applied to all systems studied followed by 100 ns of a NVT MD at 300 K. The SA consisted of two steps: first a quick heating from 300 to 500 K in 200 ps, followed by a slow cooling down from 500 to 300 K in 5 ns.

Copolymers Synthesis. All reagents were purchased in the purest available form and were used as received. Sodium hydroxide, isopropanol, and acetone were purchased from Cicarelli (Buenos Aires, Argentina). Deionized water was used for sample preparation. Thymine, 4-vinylbenzyl chloride, 2,2′-azobis-2-methylpropionitrile (AIBN), triethylamine, and 2,6-di-*tert*-butyl-4-methylphenol were purchased from Sigma-Aldrich (Buenos Aires, Argentina). Vinylbenzylthymine (VBT) was synthesized from thymine and vinylbenzyl chloride while vinylbenzyltriethylammonium (VBA) was synthesized from vinylbenzyl chloride and triethylamine as described previously.[34,35] Based on ^{1}H NMR spectra (Bruker 300 MHz) and melting point results, the monomeric products were deemed pure enough for the synthesis of the copolymers.

The copolymerization of the VBT:VBA 1:4 copolymer was performed in a round-bottom flask by a free radical process where VBT (0.041 M) and VBA (0.165 M) monomers were added to isopropanol (20.23 M) as solvent. The VBT:VBA mixture was stirred and heated to 65 °C until the solution was clear. Afterward, AIBN (0.0031 M) was added to the flask under inert N_2 atmospheric conditions, and the solution was kept at 65 °C and stirred for 16−20 h. The reaction mixture was cooled to room temperature and rotary evaporated to concentrate to 50%. The addition of the mixture to 1 L of cold acetone produced the polymer to precipitate out of the acetone/isopropanol mixture. Subsequently, the white solid precipitate was filtered and dried under vacuum. To verify the absence of unreacted monomers, the precipitated polymer was analyzed by ^{1}H NMR spectroscopy, and the typical vinyl group signal at chemical shifts between 5 and 6 ppm was not observed in the spectra. An identical procedure was followed for the VBT:VPS 1:1 copolymer, varying only the corresponding ratio of starting monomers.

Circular Dichroism. Measurements were carried out at 300 K on a Jasco 810 spectropolarimeter (Jasco Corporation, Japan) equipped with a Peltier-effect device for temperature control. The instrument was calibrated following the manufacturer's instructions. Scan speed was set to 20 nm/min with a 1 s response time, 0.2 nm data pitch, and 1 nm bandwidth. Near-UV measurements (250−350 nm) were carried out in 1.0 cm cells, while in the far-UV (180−250 nm) 0.2 cm cells were used. Three spectra were recorded and averaged for each sample.

Aqueous solutions of 1% VBT:VBA copolymers 1:1 and 1:4 were prepared and homogenized by manual stirring. Dilutions of 1:300 and 1:3000 in deionized water were used for measurements.

Atomic Force Microscopy. The morphology and geometric parameters of the VBT−VBA copolymer aggregates were determined by using a commercial Nanotec Electronic (Nanotec Electrónica S.L., Madrid, Spain) atomic force microscope (AFM) system operating in tapping mode. All AFM experiments were performed at an atmosphere pressure and room temperature. Acquisition and image processing were performed using the WS×M free software.[36]

V-shaped Olympus RC800PSA cantilevers (Olympus Corporation, Tokyo, Japan) made of silicon nitrite coated with Au/Cr on the backside for enhanced reflectivity, resonance frequency in the range of 70−90 kHz, nominal spring constant in the range of 0.05−0.1 N/m, and a radius of curvature less than 20 nm were used.

Aqueous solutions of 1% VBT:VBA copolymers 1:1 and 1:4 were prepared and homogenized by manual stirring. Dilutions of 1:300 and 1:600 in deionized water were used for measurements. Samples for AFM analysis were prepared by depositing 30 μL of copolymer solution onto HOPG (highly ordered pyrolytic graphite, SPI Supplies) substrates and dried under a flux of nitrogen for 10 s.

RESULTS AND DISCUSSION

Copolymer Shape and Stability. Both simulated copolymers showed a clear tendency to be elongated when solvated in water as shown by their radius of gyration tensor principal eigenvalues (R_g) (Figure 2). The presence of two

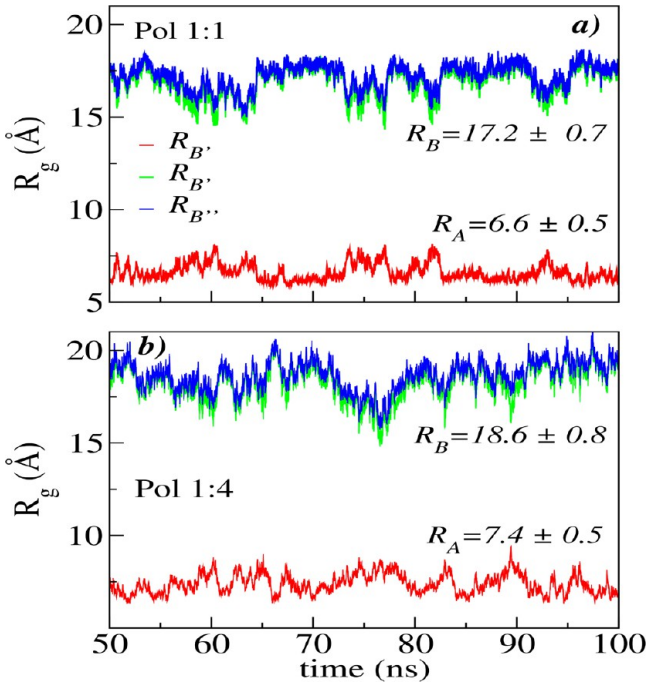

Figure 2. Time evolution of radius of gyration tensor principal eigenvalues (R_g). R_A is the time average of the smallest eigenvalue, and R_B is the time average of the two larger eigenvalues.

large and very similar radii and one small radius is typical of a prolate mass distribution with an axial symmetry axis. The stability of this property alongside the simulation time is also an indication of thermodynamic equilibrium, and it was reached after 20−30 ns in all simulations. The last 50 ns of the trajectory was assumed in thermal equilibrium and used to calculate the structural properties.

DOI: 10.1021/acs.jpcb.5b11342
J. Phys. Chem. B XXXX, XXX, XXX−XXX

R_A is the time average alongside the simulated production stage of the smallest eigenvalue, and R_B is the temporal average between the larger eigenvalues of the tensor, respectively (R_B' and R_B''). The values of these quantities are quoted in Figure 2. For Pol 1:1 it was obtained $R_B/N = 0.54 \pm 0.02$ Å, while for Pol 1:4 $R_B/N = 0.53 \pm 0.02$ Å, where N is the number of monomers in the simulated chain. The results show that the average lengths of the copolymer structure expressed by monomer are approximately the same for both species. R_A characterizes the mass distribution around the average axis of the copolymer chain, and it was found $R_A = 6.6 \pm 0.5$ Å for Pol 1:1 and $R_A = 7.4 \pm 0.5$ Å for Pol 1:4, denoting that Pol 1:4 organizes itself in a thicker structure or has larger transverse movements.

The arrival to equilibrium was also monitored by following the root mean square displacement (RMSD) of the backbone copolymer atoms after a rigid structure fitting. The temporal evolution of the RMSD indicates that their values and fluctuation magnitudes have stabilized along the final 50 ns (not shown). The RMSD temporal averages in this production stage are 4.5 ± 1.2 and 10.1 ± 2.9 Å for Pol 1:1 and 1:4, respectively. The averaged Pol 1:4 RMSD almost doubles the Pol 1:1, which agree with the facts discussed in the above paragraphs.

Larger transversal bending undulations, of wavelength in the order of the copolymer length, account for larger RMSD values for Pol 1:4 as can be seen by direct inspection of the simulation trajectories. Figure 3 shows snapshots of the simulations.

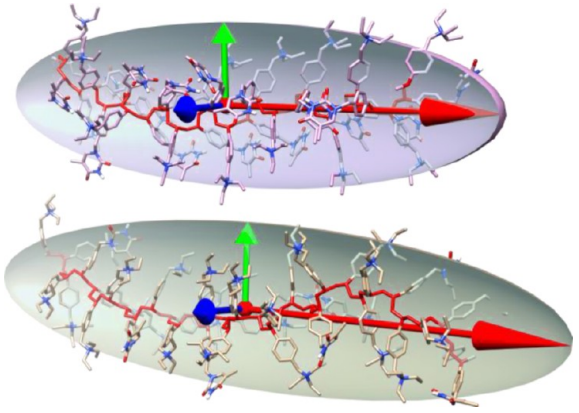

Figure 3. Snapshots from Pol 1:1 (top) and Pol 1:4 (bottom) simulations rendered with a stick representation and atoms colored with CPK code color. Their respective elongated ellipsoids were added in order to capture their approximate shape and size. The backbones of each copolymer were depicted in red.

Helicity. Several polymer fibers usually order themselves in a helical arrangement, like α-amylose, some natural polypeptides, DNA, to name a few. Among nonbiological polymer examples are the polyolefins, polymethacrylates, vinyl copolymers, polyaldehydes, and others.[37,38] Taking into account these facts, the helical shape of our copolymers was analyzed. Since the interactions that lead to the hypothetical arrangements are *a priori* unknown in our case,[39] a geometric criteria must be used and therefore a procedure based in the proposal of ref 40 was used. Three vectors between pairs of nearest-neighbor backbone carbon atoms of consecutive monomers were defined (Figure 4, yellow arrows). Consequently the difference of these consecutive vectors was calculated obtaining two new vectors

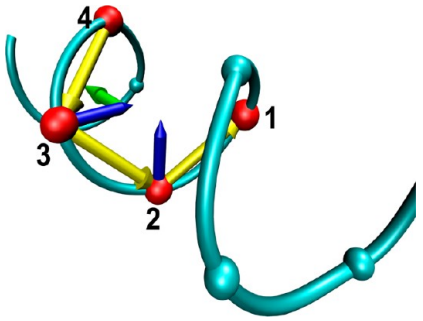

Figure 4. Schematic representation depicting the vectors used in the helix definition.

(Figure 4, blue arrows). Using the cross product of the new vectors a local axis of the structure was defined (Figure 4, green arrow). The criteria for the existence of a helical structure is that the dot product of two consecutive local axis (ζ) is close to 1. This criteria involves five consecutive atoms of the backbone. It is important to note that a copolymer of N residues has $N - 4$ helix segments defined. Our geometrical criteria were tested in proteins where the DSSP algorithm[39] is also applicable giving comparable results.

Figure 5 shows the time averaged ζ parameter with the standard deviation for each consecutive group of five monomers along the copolymer. The fraction of local segments with $\zeta \geq 0.9$ is 75% for Pol 1:1 and 54% for 1:4, respectively, showing that the helical structure extends to broader regions in

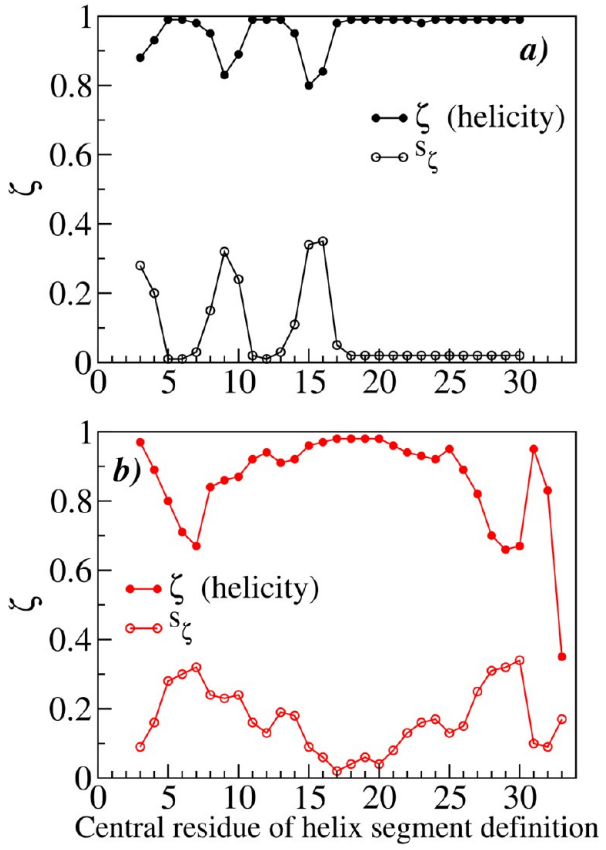

Figure 5. Time-averaged ζ parameter and the standard deviation for each consecutive group of five monomers along the copolymer: Pol 1:1 (a) and Pol 1:4 (b).

DOI: 10.1021/acs.jpcb.5b11342
J. Phys. Chem. B XXXX, XXX, XXX−XXX

the former system. The profiles in Figure 5 also show the regions of the copolymer where the helical structure is more labile. The localization of these labile zones do not correlate with the local stoichiometry of the sequence where they take place, as it is particularly evident for Pol 1:1, but also true for Pol 1:4 (see Figure 5). The reasons for the loss of helicity will be analyzed following the next section.

Assuming a relationship between the existence of local helical structures and the rigidity of the chain to bending fluctuations, the larger RMSD and R_A values for Pol 1:4 can be explained. This relation is explored in the next paragraph.

Thymine Interactions. Base stacking is a common phenomenon found either in DNA (RNA) or protein, and it has been largely studied. It is well-known that in the very first approximation base stacking can be described as a combination of the three most basic contributions to molecular interactions, namely, electrostatic interaction, London dispersion attraction, and short-range repulsion. It can be well modeled by the simplest atomistic empirical potentials consisting of the Lennard-Jones and Coulomb terms using just fixed atomic point charges localized at the geometrical centers of the atoms.[41−43]

Considering the energy components of the interaction (Coulomb and dispersion terms) between two stacked thymine moieties a geometrical criteria was used to follow the statistic of ring stacking along the simulations. It was assumed an existence of interaction if the center of mass of two thymine rings were closer than 5.5 Å and the vectors normal to their rings were almost parallel to each other (angle less than 20°). It was found that thymine stacking was one prominent way of stabilization present in the copolymers (mainly Pol 1:1). Figure 6 shows the interactions found in Pol 1:1 and 1:4 as a contact map. For Pol 1:1 the more frequent interactions are between thymine rings at sites $(i, i + 4)$. For Pol 1:4 the stacking interactions are more constrained due to the copolymer stoichiometry, presenting only $(i, i + 5)$ thymine stacking with lower probability than Pol 1:1. Since these interactions connect consecutive turns of the helix structure, they contribute to the rigidity in contradiction to the bending fluctuations and will be discussed below.

Backbone Flexibility. Root-mean-square fluctuation (RMSF) is a suitable tool to measure the size of local changes of the copolymers backbones. The average square deviations of each backbone atom referred to the same atom in the average copolymer structure obtained from the last 20 ns of the trajectories after least-squares fitting of the backbone atoms in each frame are shown in Figure 7 for both copolymers as a function of the residue index. Given that the RMSF of each monomer is determined relative to the time averaged backbone structure, the variable reflects the local mean-square displacements normal to the chain direction and therefore is a measure of the bending flexibility of the copolymer. For each monomer the symbol is drawn filled if such residue is located at the center of a segment with $\zeta \geq 0.9$, and therefore it is structured in helix to facilitate the correlation between both properties. Both copolymers have biggest fluctuations at the beginning and at the end of the chain, due to less constrained binding environment on those regions, as can be expected. In addition, the position of the peaks in the RMSF profile correlates with the location of nearby regions where the helical structure is more labile (see Figure 5), and consequently Pol 1:4 has more regions with larger fluctuations. Outsized clusters of charged monomers in Pol 1:4 reduce the enthalpic contribution, turning

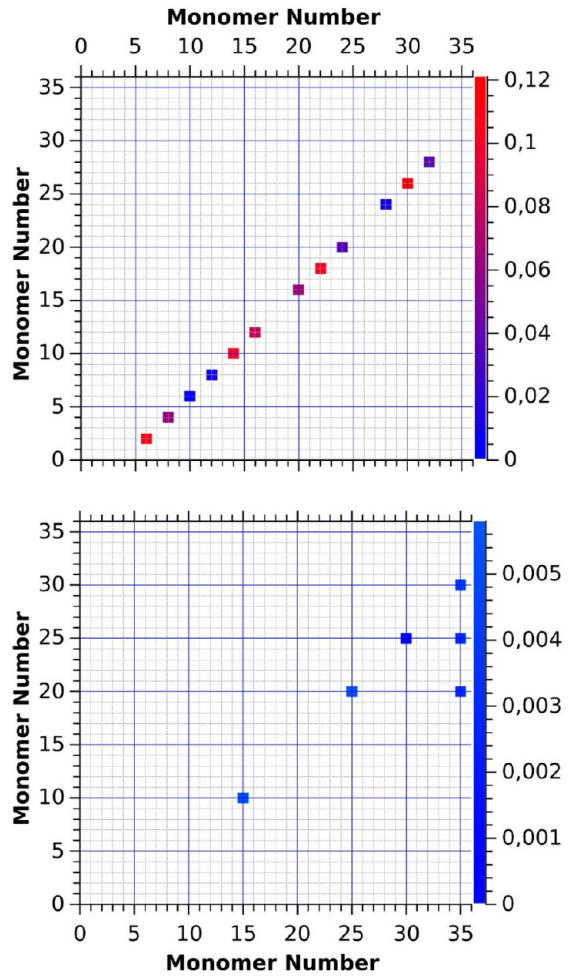

Figure 6. Contact map of the interactions found in Pol 1:1 (top) and 1:4 (bottom). The color code of each matrix element represents the frequency observed for the stacking of each monomer.

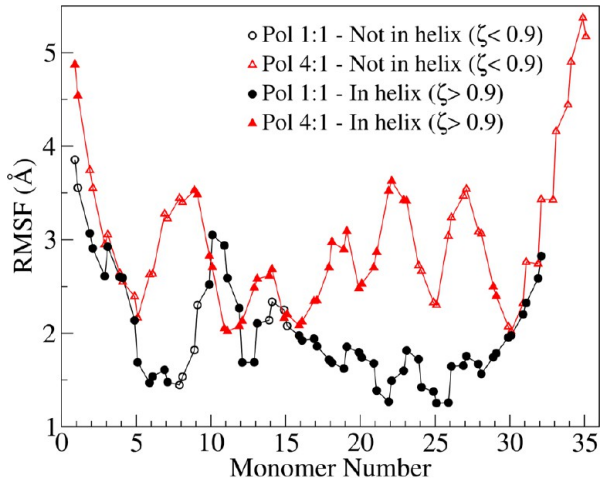

Figure 7. Root-mean-square fluctuactions (RMSF) of the backbone atoms referred to the average copolymer structure obtained from the last 20 ns of the trajectories.

indispensable the stabilization through the entropic term due to conformational variants.

Circular Dichroism Measurements. Experiments of circular dichroism of copolymers of Pol 1:1 and 1:4 molar

DOI: 10.1021/acs.jpcb.5b11342
J. Phys. Chem. B XXXX, XXX, XXX−XXX

ratio were conducted in very diluted aqueous solution, and no optical activity was registered. The typical peptide signal in the far-UV (180−220 nm) is associated with the double bond of the peptide, which does not have analogues in the copolymer systems. Regarding possible signals in the near-UV region (250−350 nm), the MD simulations showed that the frequency and features of the thymine−thymine interactions do not guarantee the occurrence of optical activity for this stoichiometry and initial copolymer molecular weight.

Side Chain Behavior. To study the order of the side chain moieties in each copolymer, a vector (V_1) between the CC1 backbone atom and CR1 benzene atom was defined. The angle between V_1 and the local helix axis of this segment (θ_B) gives information about the tilt of the benzyl moieties relative to the local longitudinal axis of the chain. Figure 8 shows the time-

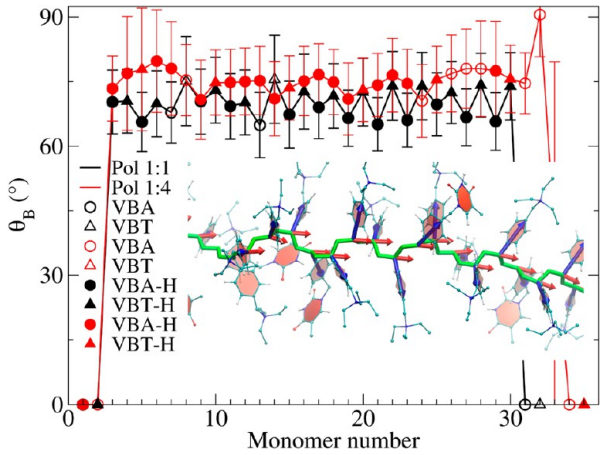

Figure 8. Residues with $\zeta \geq 0.9$ are depicted in filled symbols. VBA and VBT residues are represented with circles and triangles, respectively. The inset shows a snapshot of the simulation with the vectors whose orientations are considered. The blue and red arrows represent V_1 and central axis vectors, respectively.

averaged and standard deviation of angle θ_B as a function of the residue number for each copolymer. It can be noticed that the orientation of each benzyl moiety is slightly tilted toward the principal axis of the copolymer from the normal orientation. For Pol 1:1, the benzyl ring of the thymine monomer is closer to the normal orientation compared to the benzyl groups attached to the ammonium moieties. The average θ_B profile of Pol 1:4 shows a periodic variation consistent with the chemical composition pattern of the monomers and is closer to 90° compared to Pol 1:1. The accumulation of cationic monomers in Pol 1:4 favors arrangements with the benzyl moieties closer to the normal of the helix axis to decrease the electrostatic repulsion. The repulsive interactions between neighbors charged groups impose a stress to the structure of Pol 1:4, which is evident from the bonding energy terms in Table 2 when compared against Pol 1:1.

Table 2. Bonding Energy Terms (in kJ/mol)

	bonding interactions (temporal average per interaction type)		
	bending	dihedral	improp dihedral
Pol 1:1	2.98	8.06	4.10
Pol 1:4	4.05	10.34	8.85

Isolated Fiber Size. It was shown that the copolymer chains adopt a linear conformation in solution. Therefore, it is relevant to determine the width of such structures to compare with the diameter of fiber aggregates that can be observed experimentally. The cylindrical distribution function (CDF) of the number of atoms around the instantaneous axis of the copolymer for benzyl rings, thymine rings, and triethylammonium moieties was calculated (see Figure 9). In this calculation

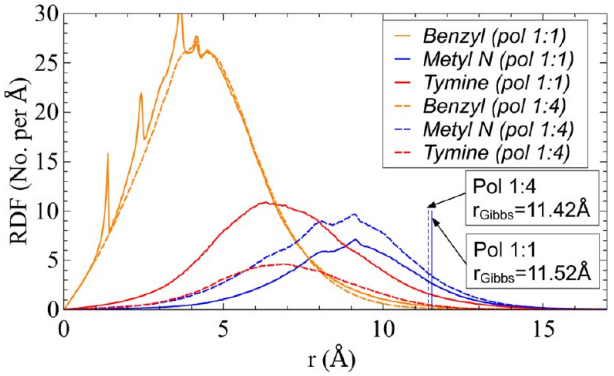

Figure 9. Cylindrical distribution function (CDF) of the number of atoms around the instantaneous axis of the copolymer for benzyl, thymine, and triethylammonium groups.

the contribution of the monomers close to the chain end were not taken into account; only the 21 central residues were considered to avoid artifacts due to the disorder of terminal regions. The criterion to define the limits of the copolymer was the Gibbs dividing surface method applied to the CDS of the most exposed moiety, the triethylammonium.[44] The radius obtained for Pol 1:1 and 1:4 was 11.5 and 11.4 Å, respectively. In order to define a width having better physical meaning, the van der Waals radii of the triethylammonium methyl terminal group (1.5 Å) was added. The diameters of the copolymer structures subsequently calculated were 2.60 and 2.58 nm for Pol 1:1 and 1:4, respectively. Considering that these diameters were calculated in water, they are influenced by the bending fluctuations of the copolymer. The magnitude of such fluctuations can be estimated to be ∼2−3 Å from the RMSF profiles (∼10% of the calculated diameters). Nevertheless, taking into account that the Gibbs criteria was used to determine the diameter of the copolymer structure from the CDF, the influence of fluctuations of this magnitude it is expected to be negligible. The presence of the HOPG substrate in the AFM experiments reduces even further such fluctuations.

Atomic Force Microscopy Measurements. AFM images of diluted water solutions of copolymers Pol 1:1 and 1:4 onto HOPG substrates are shown in Figure 10. Pseudocolor images of both copolymers were acquired after depositing copolymer samples onto recently cleaved HOPG surfaces and gently dried by a N_2 flux. The acquired data were processed using the "Gwyddion" software[45] to perform the leveling and background subtraction. Images are representative of several regions, and different samples analyzed, showing the morphology changes between both copolymerization ratios. From the images it can be noticed that the copolymer chains form fiber-like structures that interconnect among them for all the samples. Material displacements were observed in a few regions of the samples despite the fact that measurements were taken in tapping mode (see Figure 11), which is indicative that the interaction among the fibers and HOPG substrate is relatively weak.

DOI: 10.1021/acs.jpcb.5b11342
J. Phys. Chem. B XXXX, XXX, XXX−XXX

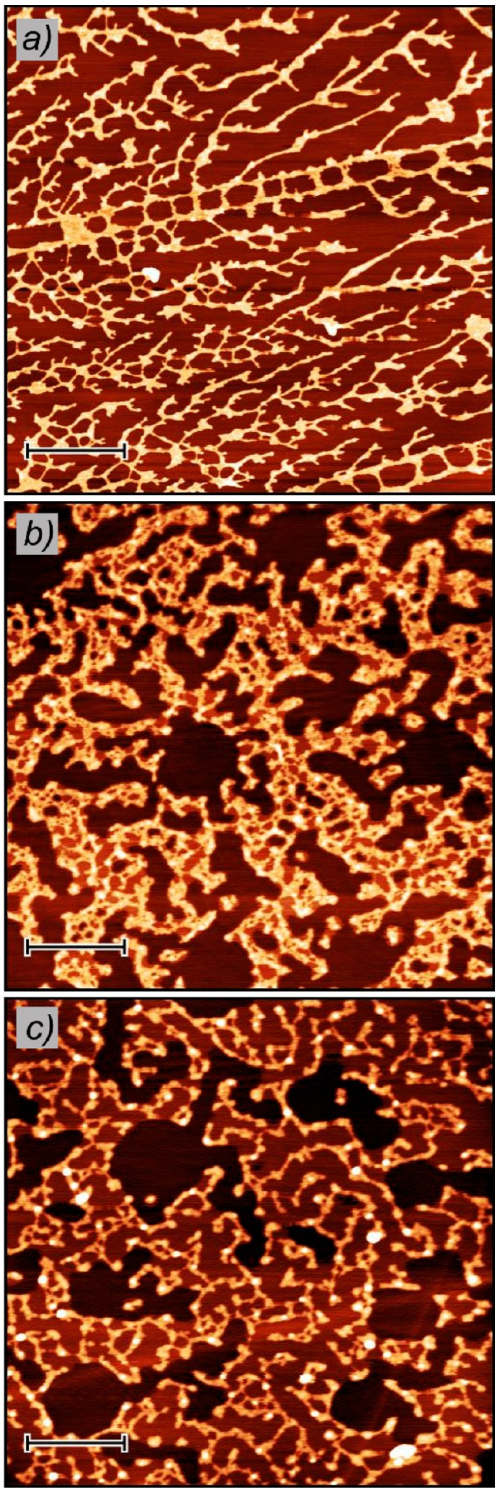

Figure 10. Topographic pseudocolor AFM images for (a) Pol 1:1 (5000 nm × 5000 nm, scale bar = 1 μm) and (b) Pol 1:4 (2000 nm × 2000 nm, scale bar = 400 nm) on HOPG substrates after drying the water solvated sample by a N_2 flux. (c) Pol 1:4 after 3.6 J/cm^2 UV irradiation (2000 nm × 2000 nm, scale bar = 400 nm).

Figure 12 shows the measured height histograms for the three samples of the systems illustrated in Figure 10. These distributions are consistent with other obtained for different samples. Each histogram was fitted to a combination of 2 or 3 Gaussian functions to characterize the features of the corresponding sample. The lowest height peak corresponds

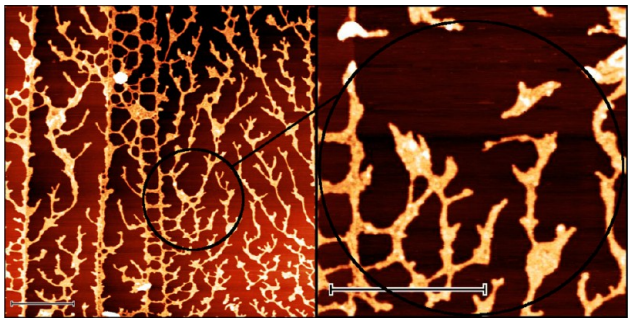

Figure 11. Topographic pseudocolor AFM images showing fiber displacements before and after scanning a smaller zone. Lengths of the scale bars are 1 μm in both images. The circles signal the zones to compare.

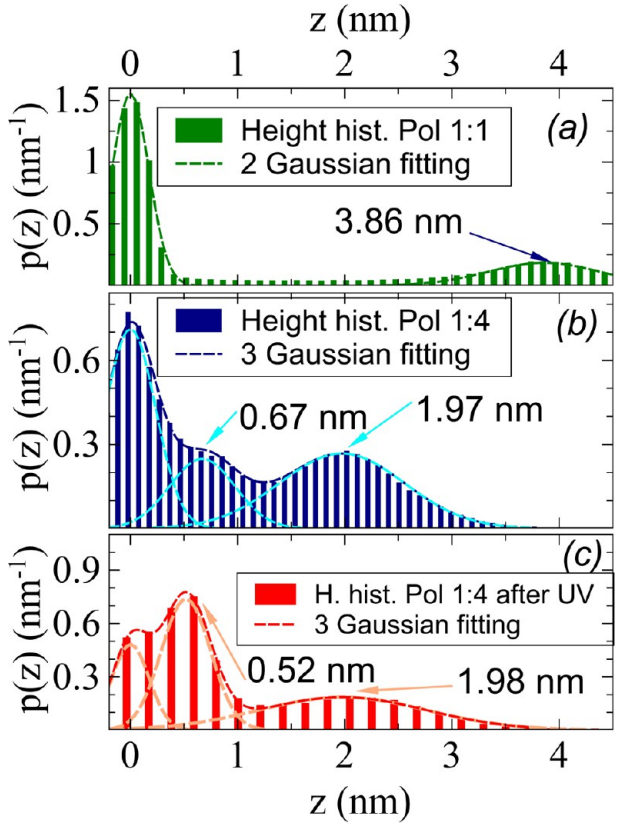

Figure 12. Fiber height histograms obtained from AFM images of (a) Pol 1:1, (b) Pol 1:4, and (c) Pol 1:4 after 3.6 J/cm^2 UV irradiation to induce the cross-linking process. Fitting curve and Gaussian function components are shown.

to HOPG substrate regions free of fibers as can be verified by analyzing the images with the appropriate thresholds. The center of the lowest Gaussian peak was defined as the origin for height measurements above the substrate.

Pol 1:1 has only one additional peak associated with the fiber thickness, with a central value of the Gaussian at 3.87 nm. Conversely Pol 1:4 has two peaks besides the substrate, the largest height peak at 1.97 nm associated with the copolymer fibers, and another peak at 0.67 nm associated with terraces that extend around or between fibers. Figure 13 presents an AFM image and the corresponding height profile. This peak can be assigned to the presence of hydrated ClNa that surround the charged copolymer in the original solution.

DOI: 10.1021/acs.jpcb.5b11342
J. Phys. Chem. B XXXX, XXX, XXX−XXX

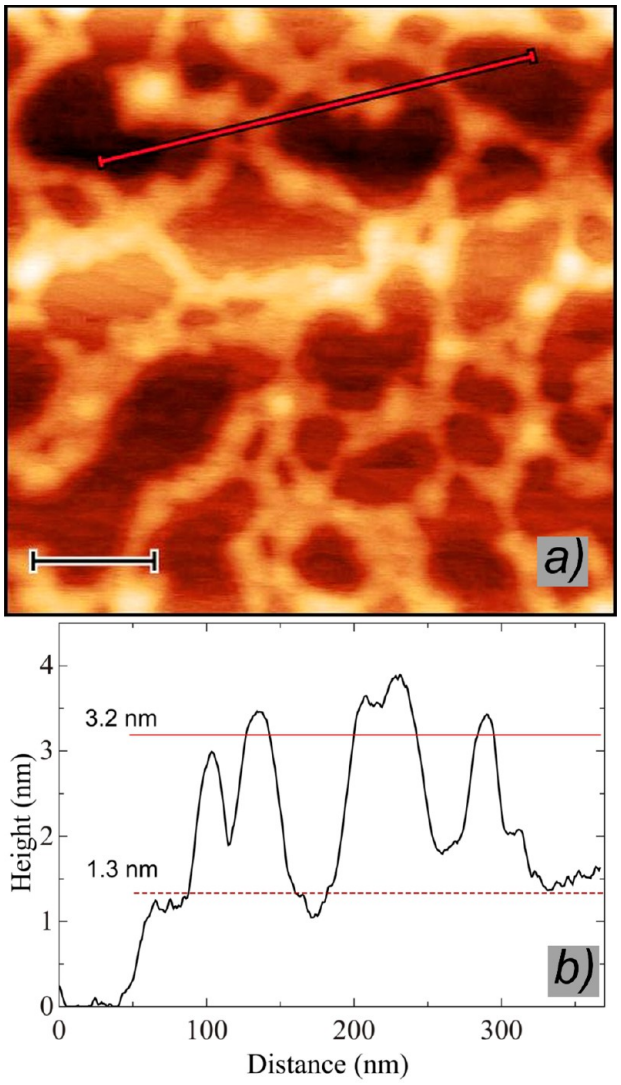

Figure 13. (a) Topographic pseudocolor AFM image of an expanded region (black scale bar = 100 nm) of Pol 1:4 and (b) the height profile along the red line in image (a).

Comparing these results with the diameters of individual copolymer chains as obtained from the simulations, 2.60 and 2.58 nm for Pol 1:1 and Pol 1:4, respectively (see Figure 9), it can be concluded that each fiber of Pol 1:1 is constructed by a bunch of two copolymer chains. On the contrary, for the copolymer Pol 1:4 each fiber is constituted by an isolated chain. The fact that Pol 1:4 has a larger charge density that Pol 1:1 could explain the presence of isolated chains for this system. A characteristic average fiber length between fiber intersections can be extracted from the analysis of the images also.[46] Their values are 189 and 75 nm for Pol 1:1 and 1:4, respectively.

AFM measurements of the Pol 1:4 system were carried out after illuminating the samples with 3.6 J/cm^2 doses of UV radiation to induce the cross-linking reactions between copolymer chains. Figure 12c shows in red bars the histogram of Pol 1:4 after UV irradiation, presenting a distribution very similar to the unirradiated sample of Pol 1:4. In order to obtain appropriated AFM images that allow for the measurement of the individual fiber thickness, highly diluted samples were used. In this limit the surface coverage of the substrate is unobtrusive and the average distance between thymine groups of adjacent fibers is large enough to prevent the cross-linking reactions among Pol 1:4 chains. Therefore, the UV irradiation dose applied did not change the distribution of fiber diameters.

Two-Copolymer-Chain Interaction. In the cross-linking reaction between copolymer chains occurring when illuminating with ultraviolet radiation, the proximity among chains is a critical issue. Therefore, it is important to understand the process that lead to such proximity despite of the Coulomb repulsion between equally charged chains. The association of polyelectrolyte polymers is also a well-known phenomena, particularly in biology and is relevant to analyze for the present case in view of the AFM results.[15] The association or even the condensation of polyelectrolyte chains is mediated by the counterions. It has been established that the condensation of like-charged polymer chains cannot be explained theoretically by mean field approximation theories since it involves correlations among counterions and the building of nanoscale arrangements.[47] Small-angle X-ray and synchrotron radiation measurements have shown that attractive forces among the polyelectrolyte mediated by the counterions led to the formation of condensed phases.[15] MD simulations were implemented for two copolymers solvated in a simulation box with water and the counterions that cancel their charges, named as the intrinsic counterion ionic strength. Nevertheless, results from simulations under higher ionic concentrations that can be also relevant are not presented.

In these MD simulations with pairs of the copolymers chains Pol 1:1 and 1:4 the minimum distance between chains grew from the initial configuration along the simulated time until they reached a stationary value (minimum averaged distance during the last 10 ns of simulation D_{P-P} = 48 ± 7 Å). Nevertheless, at the stationary configurations the minimum distances between the chains in the central simulation box is greater than between those chains and the ones in periodic images. Consequently, it was suspected that coupled chains do not arrive to stable equilibrium pair configurations. To confirm this, hypothesis binding energy between chains was estimated taking into account the average values of electrostatic interactions including copolymer−copolymer, copolymer−water, copolymer−ions, ions−ions, and water−water once the simulations reached the stationary configuration. Negative values of the binding energy between chains for both copolymer species were found reinforcing that the simulated chains do not bind at the intrinsic ionic strength analyzed in this work.

Despite this conclusion, the following features in the arrangements of the copolymer chains at stationary conditions were observed. The principal axis of the copolymers chains arrange in collinear (terminus-to-terminus) or perpendicular relative orientations to minimize the electrostatic repulsion. This tendency is in agreement with what have been found in experimental and theoretical studies of charged polymers.[11]

To characterize the counterion distribution, we calculate the average number of charged atoms in shells defined considering a constant distance from the surface of the copolymer chain. The shells were implemented by taking small bin intervals of this distance. The black dotted curve in Figure 14 shows the counterion distribution as a function of distance for an isolated Pol 1:1 simulation. The red dotted curve shows the number of counterions distribution around one copolymer for two Pol 1:1 simulation. A crude approximation to analyze the ion accumulation between the copolymers for both simulated systems is as follows. The distribution curve of a second

DOI: 10.1021/acs.jpcb.5b11342
J. Phys. Chem. B XXXX, XXX, XXX−XXX

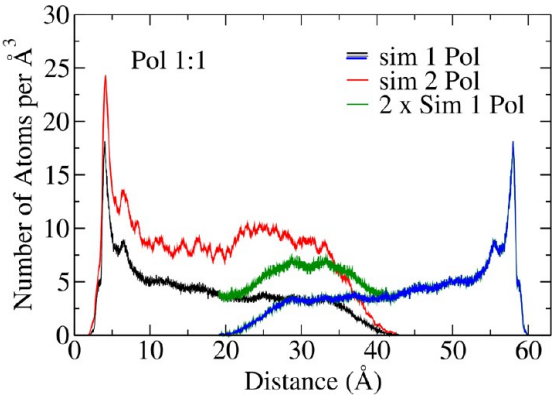

Figure 14. Radial distribution function of chloride atoms from the surface of each copolymer, calculated for system 1:1 with one and two copolymers in the simulation periodic box.

isolated copolymer (blue curve) positioned at the average distance between copolymers in the high concentration system was plotted. The sum of the last two curves (green dots) was compared to the result from the two-copolymer simulation as an approximation to detect the chlorine accumulation among them. Figure 14 shows that the number of chlorine ions at mid distances between copolymers is higher for the two-copolymer simulation than the sum of ions from two isolated systems. This fact indicates the presence of an accumulation of ions between the copolymers. Similar results were obtained for the Pol 1:4 systems (results not shown). Antila and Sammalkorpi[11] showed that in DNA simulations when only counterions were present they do not accumulate close to the macromolecule, and therefore they did not produce charge inversion at short distances from the copolymer. This result is in agreement with our simulations where counterions tend to locate between both copolymers, but not close to them. The lack of charge inversion at short distance in our simulation explains why the copolymers repel each other, and they arrange themselves in collinear or perpendicular arrangements. Chialvo and Simonson[10] showed by MD simulations that the addition of salts beyond the intrinsic ionic condition decrease the effective charge of short polyelectrolytes of polystyrenesulfonate even reaching the charge neutrality. They also found that the counterions association depends on the total charge of the polyelectrolyte but is not sensible to the sequence of the charged sulfonate groups in the chains. The dependency of the polyelectrolytes association on the ionic strength and the counterion specie has also been establish.[47] Nevertheless, as discussed above the condition of attraction between equally charged polyelectrolytes to favor their condensation requires of nanoscale length chains,[47] and this limit is beyond the scope of the present MD simulations.

The counterion concentration appears to be due to fine interplay between the electrostatic attraction of a counterion to a copolymer chain and the loss of the translational entropy by counterions due to their localization in the vicinity of the copolymer chain. In a very dilute polyelectrolyte solution the entropic drawback for counterion condensation is very high, and almost all counterions leave copolymer chains and stay "free" in the solution. However, as copolymer concentration increases, the entropic disadvantage for counterion localization decreases, resulting in a gradual increase in the counterion density between the copolymer. The local distribution of counterions around the copolymers will be a fundamental force to get the fibers close enough to be able to cross-link by UV irradiation.

CONCLUSIONS

The structure of isolated finite length chains of the VBT−VBA copolymers in 1:1 and 1:4 monomer ratios solvated in water was studied with the aid of molecular dynamics simulations. The results allowed the determination of the width of the copolymer structures and the basic interactions that lead to these arrangements. To the best of our knowledge, this is the first simulation of VBT−VBA copolymers at the atomistic scale. Therefore, we also report the force field parameters for the simulation of VBT and VBA monomers in these copolymers.

The thickness of the fibers for copolymer Pol 1:4 measured by AFM are consistent with the hypothesis that they are isolated copolymer chains. Conversely, the fiber thicknesses measured for Pol 1:1, that doubled the values for copolymer Pol 1:4 ratio, give evidence of the association in a pair of chains. At the ionic strength used in our samples, the ion concentration is enough to induce the association of Pol 1:1 chains, but not in the case of Pol 1:4 which had a higher concentration of charge. Therefore, the phenomena of charge inversion is likely to be present for the Pol 1:1 system under the present experimental conditions[11] but not for Pol 1:4. The association of chains in bunches and the large probability of intrachain *i*, *i* + 4 thymine−thymine stabilizing interactions favor fibers of large curvature radii (see Figure 10a) for Pol 1:1. The higher charge density of Pol 1:4 gives rise to isolated copolymer chains for this system, which together with a lower prevalence of thymine−thymine intrachain stacking explains the smaller thickness and larger curvature of their fibers (see Figures 10b and 10c). The systematic study of the copolymer chain aggregation as a function of ion concentration is beyond the scope of the present work. Nevertheless, the methods and results presented here are appropriate to conduct such investigations.

AUTHOR INFORMATION

Corresponding Author

*E-mail daniel.rodrigues@dfbioq.unl.edu.ar; Phone/Fax +54(342) 4575-213 (D.E.R.).

Notes

The authors declare no competing financial interest.

ACKNOWLEDGMENTS

Authors acknowledge the use of the computational facilities of the FaCAP (Facilidad de Computación de Alta Performance) at the Facultad de Bioquímica y Ciencias Biológicas, Universidad Nacional del Litoral, Argentina, and thank the financial support of CONICET (PIP-2012-0895 and -0577); UNL-CAID 2012 (No. 501 201101-00040, -00093, and -00283 LI). D.E.R., D.M.M., and M.C.G.P. are members of the Consejo Nacional de Investigaciones Científicas y Técnicas (CONICET), Argentina.

REFERENCES

(1) Martino, D. M.; Reyna, D.; Estenoz, D. A.; Trakhtenberg, S.; Warner, J. C. Photosensitization of Bioinspired Thymine-Containing Polymers. *J. Phys. Chem. A* **2008**, *112*, 4786−4792.

(2) Barbarini, A. L.; Estenoz, D. A.; Martino, D. M. Synthesis, Characterization and Curing of Bioinspired Polymers Based on Vinyl Benzyl Thymine and Triethyl Ammonium Chloride. *Macromol. React. Eng.* **2010**, *4*, 453−459.

DOI: 10.1021/acs.jpcb.5b11342
J. Phys. Chem. B XXXX, XXX, XXX−XXX

(3) Ledesma, J.; Bortolato, S. A.; Boschetti, C. E.; Martino, D. M. Optimization of Environmentally Benign Polymers Based on Thymine and Polyvinyl Sulfonate Using Plackett-Burman Design and Surface Response. *J. Chem.* **2013**, *2013*, 947137.
(4) Andrey, V.; Dobrynin, M. R. Theory of Polyelectrolytes in Solutions and at Surfaces. *Prog. Polym. Sci.* **2005**, *30*, 1049−1118.
(5) Liao, Q.; Dobrynin, A. V.; Rubinstein, M. Molecular Dynamics Simulations of Polyelectrolyte Solutions: Nonuniform Stretching of Chains and Scaling Behavior. *Macromolecules* **2003**, *36*, 3386−3398.
(6) Wang, L.; Brown, S. J. BindN: A Web-Based Tool for Efficient Prediction of DNA and RNA Binding Sites in Amino Acid Sequences. *Nucleic Acids Res.* **2006**, *34*, W243−W248.
(7) Liao, Q.; Dobrynin, A. V.; Rubinstein, M. Molecular Dynamics Simulations of Polyelectrolyte Solutions: Osmotic Coefficient and Counterion Condensation. *Macromolecules* **2003**, *36*, 3399−3410.
(8) Chang, R.; Yethiraj, A. Dilute Solutions of Strongly Charged Flexible Polyelectrolytes in Poor Solvents: Molecular Dynamics Simulations with Explicit Solvent. *Macromolecules* **2006**, *39*, 821−828.
(9) Micka, U.; Holm, C.; Kremer, K. Strongly Charged, Flexible Polyelectrolytes in Poor Solvents: Molecular Dynamics Simulations †. *Langmuir* **1999**, *15*, 4033−4044.
(10) Chialvo, A. A.; Simonson, J. M. Solvation Behavior of Short-Chain Polystyrene Sulfonate in Aqueous Electrolyte Solutions: A Molecular Dynamics Study. *J. Phys. Chem. B* **2005**, *109*, 23031−23042.
(11) Antila, H. S.; Sammalkorpi, M. Polyelectrolyte Decomplexation via Addition of Salt: Charge Correlation Driven Zipper. *J. Phys. Chem. B* **2014**, *118*, 3226−3234.
(12) Carrillo, J.-M. Y.; Dobrynin, A. V. Detailed Molecular Dynamics Simulations of a Model NaPSS in Water. *J. Phys. Chem. B* **2010**, *114*, 9391−9399.
(13) Lee, H.; Venable, R. M.; MacKerell, A. D.; Pastor, R. W. Molecular Dynamics Studies of Polyethylene Oxide and Polyethylene Glycol: Hydrodynamic Radius and Shape Anisotropy. *Biophys. J.* **2008**, *95*, 1590−1599.
(14) Borodin, O.; Smith, G. D.; Bandyopadhyaya, R.; Byutner, O. Molecular Dynamics Study of the Influence of Solid Interfaces on Poly(ethylene Oxide) Structure and Dynamics. *Macromolecules* **2003**, *36*, 7873−7883.
(15) Wong, G. C. L.; Pollack, L. Electrostatics of Strongly Charged Biological Polymers: Ion-Mediated Interactions and Self-Organization in Nucleic Acids and Proteins. *Annu. Rev. Phys. Chem.* **2010**, *61*, 171−189.
(16) Dobrynin, A. V. Theory and Simulations of Charged Polymers: From Solution Properties to Polymeric Nanomaterials. *Curr. Opin. Colloid Interface Sci.* **2008**, *13*, 376−388.
(17) Wang, D.; Yuan, Y.; Mardiyati, Y.; Bubeck, C.; Koynov, K. From Single Chains to Aggregates, How Conjugated Polymers Behave in Dilute Solutions. *Macromolecules* **2013**, *46*, 6217−6224.
(18) Ponder, J. W.; Richards, F. M. An Efficient Newton-like Method for Molecular Mechanics Energy Minimization of Large Molecules. *J. Comput. Chem.* **1987**, *8*, 1016−1024.
(19) Allinger, N. L. Conformational Analysis. 130. MM2. A Hydrocarbon Force Field Utilizing V1 and V2 Torsional Terms. *J. Am. Chem. Soc.* **1977**, *99*, 8127−8134.
(20) Schmidt, M.; Baldridge, K.; Boatz, J.; Elbert, S.; Gordon, M.; Jensen, J.; Koseki, S.; Matsunaga, N.; Nguyen, K.; Su, S.; et al. General Atomic and Molecular Electronic Structure System. *J. Comput. Chem.* **1993**, *14*, 1347−1363.
(21) Cornell, W. D.; Cieplak, P.; Bayly, C. I.; Kollmann, P. A. Application of RESP Charges to Calculate Conformational Energies, Hydrogen Bond Energies, and Free Energies of Solvation. *J. Am. Chem. Soc.* **1993**, *115*, 9620−9631.
(22) Oostenbrink, C.; Villa, A.; Mark, A. E.; Van Gunsteren, W. F. A Biomolecular Force Field Based on the Free Enthalpy of Hydration and Solvation: The GROMOS Force-Field Parameter Sets 53A5 and 53A6. *J. Comput. Chem.* **2004**, *25*, 1656−1676.
(23) Chiu, S. W.; Clark, M.; Balaji, V.; Subramaniam, S.; Scott, H. L.; Jakobsson, E. Incorporation of Surface Tension into Molecular Dynamics Simulation of an Interface: A Fluid Phase Lipid Bilayer Membrane. *Biophys. J.* **1995**, *69*, 1230−1245.
(24) Berendsen, H. J. C.; van der Spoel, D.; van Drunen, R. GROMACS: A Message-Passing Parallel Molecular Dynamics Implementation. *Comput. Phys. Commun.* **1995**, *91*, 43−56.
(25) Van Der Spoel, D.; Lindahl, E.; Hess, B.; Groenhof, G.; Mark, A. E.; Berendsen, H. J. C. GROMACS: Fast, Flexible, and Free. *J. Comput. Chem.* **2005**, *26*, 1701−1718.
(26) Pronk, S.; Páll, S.; Schulz, R.; Larsson, P.; Bjelkmar, P.; Apostolov, R.; Shirts, M. R.; Smith, J. C.; Kasson, P. M.; van der Spoel, D.; et al. GROMACS 4.5: A High-Throughput and Highly Parallel Open Source Molecular Simulation Toolkit. *Bioinformatics* **2013**, *29*, 845−854.
(27) Darden, T.; York, D.; Pedersen, L. Particle Mesh Ewald: An N·log(N) Method for Ewald Sums in Large Systems. *J. Chem. Phys.* **1993**, *98*, 10089.
(28) Berendsen, H. J. C.; Postma, J. P. M.; van Gunsteren, W. F.; DiNola, A.; Haak, J. R. Molecular Dynamics with Coupling to an External Bath. *J. Chem. Phys.* **1984**, *81*, 3684.
(29) Hess, B.; Kutzner, C.; van der Spoel, D.; Lindahl, E. GROMACS 4: Algorithms for Highly Efficient, Load-Balanced, and Scalable Molecular Simulation. *J. Chem. Theory Comput.* **2008**, *4*, 435−447.
(30) Miyamoto, S.; Kollman, P. A. Settle: An Analytical Version of the SHAKE and RATTLE Algorithm for Rigid Water Models. *J. Comput. Chem.* **1992**, *13*, 952−962.
(31) Herman, J. C.; Berendsen, J. P. M. P. Interaction Models for Water in Relation to Protein Hydration. In *Intermolecular Forces*; Springer: 1981; pp 331−342.
(32) Humphrey, W.; Dalke, A.; Schulten, K. VMD: Visual Molecular Dynamics. *J. Mol. Graphics* **1996**, *14*, 33−38.
(33) Casis, N.; Luciani, C. V.; Vich Berlanga, J.; Estenoz, D. A.; Martino, D. M.; Meira, G. R. Synthesis of "bioinspired" Copolymers: Experimental and Theoretical Investigation on Poly(vinyl Benzyl Thymine-Co-Triethyl Ammonium Chloride). *Green Chem. Lett. Rev.* **2007**, *1*, 65−72.
(34) Cheng, C. M.; Egbe, M. I.; Grasshoff, J. M.; Guarrera, D. J.; Pai, R. P.; Warner, J. C.; Taylor, L. D. Synthesis of 1-(vinylbenzyl)thymine, a Novel, Versatile Multi-Functional Monomer. *J. Polym. Sci., Part A: Polym. Chem.* **1995**, *33*, 2515−2519.
(35) Zarras, P.; Vogl, O. Polycationic Salts. 3. Synthesis, Styrene Based Trialkylammonium Salts and Their Polymerization1−2 1, 2. *J. Macromol. Sci., Part A: Pure Appl. Chem.* **2000**, *37*, 817−840.
(36) Horcas, I.; Fernández, R.; Gómez-Rodríguez, J. M.; Colchero, J.; Gómez-Herrero, J.; Baro, A. M. WSXM: A Software for Scanning Probe Microscopy and a Tool for Nanotechnology. *Rev. Sci. Instrum.* **2007**, *78*, 013705.
(37) Yashima, E. Synthesis and Structure Determination of Helical Polymers. *Polym. J.* **2010**, *42*, 3−16.
(38) Nakano, T.; Okamoto, Y. Synthetic Helical Polymers: Conformation and Function. *Chem. Rev.* **2001**, *101*, 4013−4038.
(39) Kabsch, W.; Sander, C. Dictionary of Protein Secondary Structure: Pattern Recognition of Hydrogen-Bonded and Geometrical Features. *Biopolymers* **1983**, *22*, 2577−2637.
(40) Kahn, P. C. Defining the Axis of a Helix. *Comput. Chem.* **1989**, *13*, 185−189.
(41) Sponer, J.; Leszczynski, J.; Hobza, P. Electronic Properties, Hydrogen Bonding, Stacking, and Cation Binding of DNA and RNA Bases. *Biopolymers* **2001**, *61*, 3−31.
(42) Sponer, J.; Berger, I.; Spačková, N.; Leszczynski, J.; Hobza, P. Aromatic Base Stacking in DNA: From Ab Initio Calculations to Molecular Dynamics Simulations. *J. Biomol. Struct. Dyn.* **2000**, *17* (Suppl. 1), 1−24.
(43) Sponer, J.; Sponer, J. E.; Mládek, A.; Jurečka, P.; Banáš, P.; Otyepka, M. Nature and Magnitude of Aromatic Base Stacking in DNA and RNA: Quantum Chemistry, Molecular Mechanics, and Experiment. *Biopolymers* **2013**, *99*, 978−988.
(44) Curgul, S.; Van Vliet, K. J.; Rutledge, G. C. Molecular Dynamics Simulation of Size-Dependent Structural and Thermal Properties of Polymer Nanofibers. *Macromolecules* **2007**, *40*, 8483−8489.

DOI: 10.1021/acs.jpcb.5b11342
J. Phys. Chem. B XXXX, XXX, XXX−XXX

(45) Nečas, D.; Klapetek, P. Gwyddion: An Open-Source Software for SPM Data Analysis. *Cent. Eur. J. Phys.* **2011**, *10*, 181−188.
(46) Hotaling, N. A.; Bharti, K.; Kriel, H.; Simon, C. G. DiameterJ: A Validated Open Source Nanofiber Diameter Measurement Tool. *Biomaterials* **2015**, *61*, 327−338.
(47) Angelini, T. E.; Liang, H.; Wriggers, W.; Wong, G. C. L. Like-Charge Attraction between Polyelectrolytes Induced by Counterion Charge Density Waves. *Proc. Natl. Acad. Sci. U. S. A.* **2003**, *100*, 8634−8637.

DOI: 10.1021/acs.jpcb.5b11342
J. Phys. Chem. B XXXX, XXX, XXX−XXX